Journal of Photochemistry and Photobiology A: Chemistry 216 (2010) 104–109

Contents lists available at ScienceDirect

Journal of Photochemistry and Photobiology A: Chemistry

journal homepage: www.elsevier.com/locate/jphotochem

Tandem dye-sensitized solar cells consisting of floating electrode in one cell

Kenshiro Uzaki, Shyam S. Pandey, Shuzi Hayase*

Graduate School of Life Science and Systems Engineering, Kyushu Institute of Technology, 2-4 Hibikino, Wakamatsu-ku, Kitakyushu 808-0196, Japan

ARTICLE INFO

Article history:
Available online 4 August 2010

Keywords:
Dye-sensitized solar cells
Tandem
Mesh
Floating electrode

ABSTRACT

Tandem dye-sensitized solar cells (Cell TAN) consisting of a floating electrode (bottom cell) and a TiO_2 electrode prepared on a F-doped SnO_2 glass (top cell) are reported. The floating electrode is a flexible and self-standing composite film consisting of a porous titania/dye layer supported by a mesh electrode. The floating electrode was inserted between the TiO_2 electrode and the counter electrode in a conventional single dye-sensitized solar cell to fabricate the Cell TAN. Therefore, the Cell TAN is completely different from previously reported tandem cells where two cells are merely accumulated and connected to each other. The Incident Photon to Current Conversion Efficiency (IPCE) curve for the Cell TAN had two peaks corresponding to those of the two single cells. The open circuit voltage (V_{oc}) of the Cell TAN (0.88 V) was higher than that of the corresponding single cell (0.6–0.66 V). These two results strongly demonstrated that the Cell TAN has a potential for tandem cells.

1. Introduction

Efficiency of dye-sensitized solar cells is now more than 10%, which is almost the same as those of amorphous Si type solar cells [1,2]. However, the efficiency is still lower than those of other solar cells. Many trials to increase the efficiency are being done. One approach is to improve light harvesting properties by dyes covering a wide range of wavelengths [3–12]. Tandem cell is another approach to increase photovoltaic performances. There are several reports on tandem cells where two single cells are merely piled up [13–15]. For example, it has been reported that a photovoltaic tandem cell comprising a nanocrystalline dye-sensitized solar cell as a top cell for high-energy photons and a copper indium gallium selenide thin-film bottom cell for lower energy photons produces AM 1.5 solar to electric conversion efficiencies greater than 15% [13]. A tandem cell consisting of a top cell (FTO glass/TiO_2 stained by a Ru dye (N719)/electrolyte layer/FTO glasses) and a bottom cell (FTO glass/TiO_2 stained by a Ru dye (Black dye)/electrolyte layer/FTO glasses) has been reported [14]. However, these cells are not practical because they need more than three transparent conductive layered glasses. Tandem or hybrid cells having two metal oxide electrodes in one cell have been reported, where the two metal oxide layers were stained with different dyes [16–19]. A hybrid cell consisting of a top electrode (FTO glass/TiO_2 layer stained with N3)/electrolyte/Pt mesh electrode/electrolyte/a bottom electrode (TiO_2 stained with black dye)/FTO glass has been reported. The Pt electrode is inserted in an electrolyte layer between the top electrode and the bottom electrode. These two titania electrodes were connected in parallel [16]. A tandem cell consisting of a top electrode (FTO glass/TiO_2 stained by N3) and a bottom electrode (NiO stained by Erythrosin B/FTO glass) has been reported [18,19]. In these tandem cells, the bottom electrode was fabricated on the counter electrode. We now propose a new tandem cell which consists of a flexible and self-standing floating electrode working as a bottom electrode. Tandem cells can be prepared easily by using the floating electrode, namely, by inserting the floating electrode into an electrolyte layer in a conventional dye-sensitized solar cell.

2. Experimental

The cell structure and the working principle are shown in Figs. 1 and 2. The detail is described in Section 3. A top electrode (top electrode T) was fabricated by a conventional method [20]. Titania paste (Ti-Nanoxide HT, Solaronix) was coated on a F-doped SnO_2 layered glass, and the substrate was baked at 450 °C for 1 h. The Ti-Nanoxide HT did not consist of light-scattering particles so that solar light would reach the bottom electrode (bottom electrode B) effectively. The thickness of the titania layer was 5 μm. The substrate was dipped in a dye solution (a model dye: Dye 2 (Fig. 3) covering shorter wavelength (λ_{max} 429 nm)) for 1 h. Bottom electrode B was prepared by coating titania paste (Titania D, Solaronix) on a stainless mesh sheet (diameter of the stainless wire: 25 μm, thickness: 40 μm, space between these stainless wire: 25 μm, product of ASADA, Japan) [21]. The stainless wire was protected with a TiO_x thin layer, where x changed from 0 to 2 gradually from the position contacting stainless wire surface to that contacting the surface of a porous titania layer [17]. This TiO_x

* Corresponding author.
E-mail address: hayase@life.kyutech.ac.jp (S. Hayase).

1010-6030/$ – see front matter © 2010 Elsevier B.V. All rights reserved.
doi:10.1016/j.jphotochem.2010.07.025

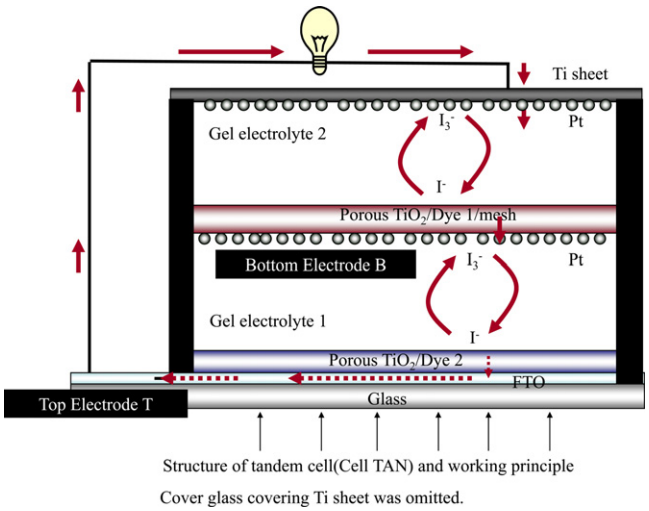

Fig. 1. Structure of tandem cell (Cell TAN) and working principle. Cover glass covering Ti sheet was omitted.

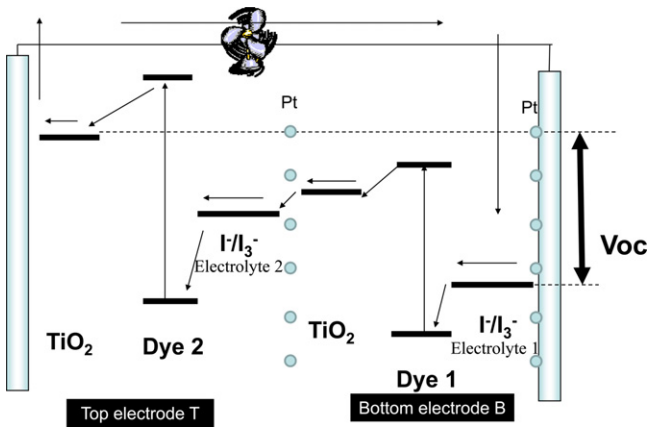

Fig. 2. Working principle of tandem cell (Cell TAN).

thin layer has a gradient structure and effectively blocked charge recombination between the stainless steel surface and iodine in an electrolyte [17]. In addition, this thin layer would protect stainless steel wires from corrosion by redox species. The gradient structure was fabricated by Ti sputtering (ULVAC Model: SH-250), followed by arc-plasma deposition (ULVAC Model: ZB04-8013) using a Ti target by the method described in our previous report [17]. The surface of the bottom electrode B was sprayed by ethanol solution of tetra(i-propoxy) titanium in order to prepare a dense TiO_2 layer on the surface of the bottom electrode B facing gel electrolyte 1. The bottom electrode B was baked at 450 °C for 1 h. Pt layer was deposited on the surface of the dense titania thin layer in the bottom electrode B by Pt-sputtering (ULVAC Model: SH-250). The thickness of the Pt layer was varied. Then, bottom electrode B was stained by dipping the substrate into a dye solution (Dye 1, Fig. 3) covering long wavelength (λ_{max} 646 nm) for 1 h. The thickness of the porous titania varied from several μm to 25 μm, depending on the position of the sheet (see cross-section view in Fig. 5). The top electrode T, a gel electrolyte sheet 1, the floating electrode (bottom electrode B), a gel electrode sheet 2, a counter electrode (Pt-sputtered Ti sheet, NILAKO, t: 100 μm), and a cover glass (thickness: 1 mm) were merely piled up to prepare the tandem cell (Cell TAN) as shown in Fig. 4. Fig. 5 shows the cross-section view of the bottom electrode B. The diameter of the stainless steel wire was 25 μm and the space between the stainless wires was completely buried with titania nano-particles. Titania particles were present on the surface of the stainless steel wires. This makes it possible for the porous titania layer to generate electrons on the whole bottom electrode B. Model dyes 1 and 2 (Fig. 3) were not high-efficiency dye molecules. They were selected because

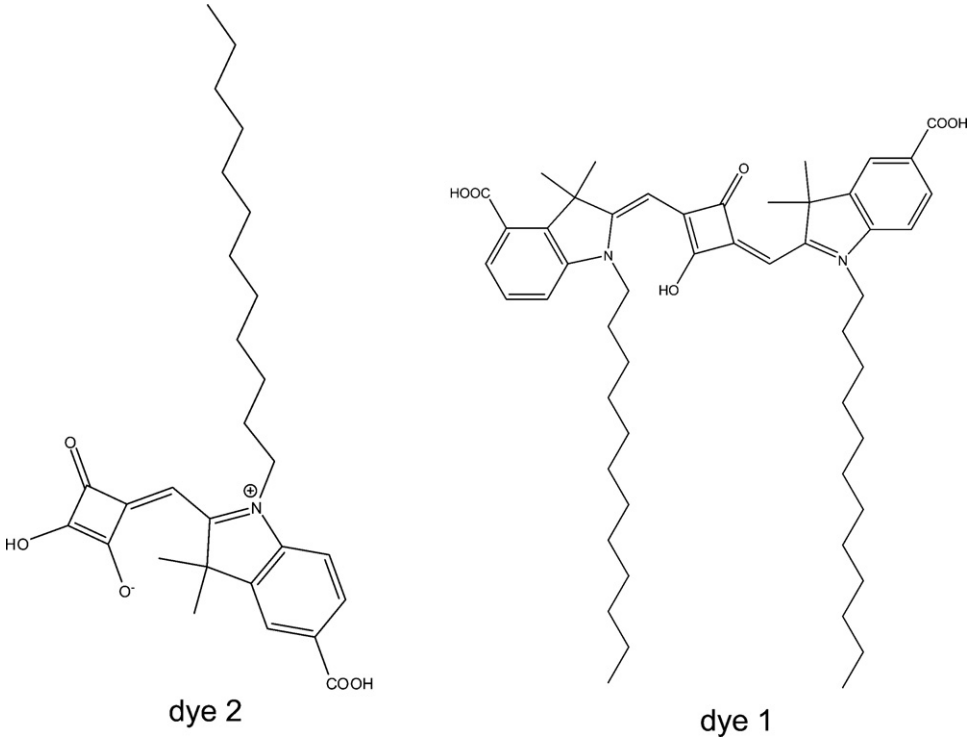

Fig. 3. Model dye structures of dye 1 and dye 2.

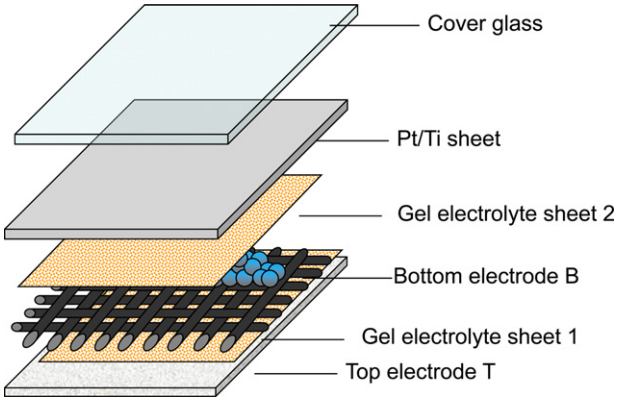

Fig. 4. Fabrication of Cell TAN.

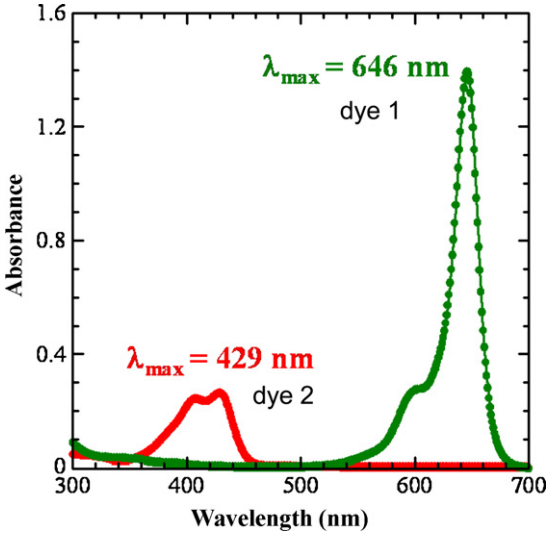

Fig. 6. Absorption spectra for dye 1 and dye 2.

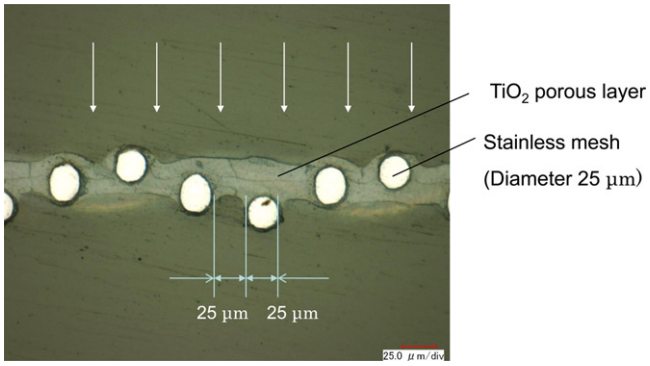

Fig. 5. Cross-section of self-standing floating electrode (bottom electrode B).

their visible absorptions did not overlap each other, namely, 429 nm for Dye 2 and 646 nm for Dye 1. This simplified analysis of the tandem properties because the absorption of the top electrode T was not affected by that of the bottom electrode B as shown in Fig. 6. Gel electrolytes 1 and 2 had same compositions and were prepared by infiltrating electrolyte C in a porous polymer sheet (Membrane filter, PTFE, HO1A293D, ADVANTEC, t: 0.1 μm). The electrolyte C consists of 500 mM of LiI, 50 mM of I_2, 600 mM of ethylmethylimidazolium dicyanamide (EtMeImN$(CN)_2$), and 580 mM of t-bupyridine (t-Bupy) in acetonitrile. Two single cells were prepared as reference cells for the Cell TAN. Cell SIN 2 shown in Fig. 7A was prepared by assembling a top electrode T, a gel electrolyte sheet 1, a counter Ti sheet electrode with Pt and a glass cover. Cell SIN 1

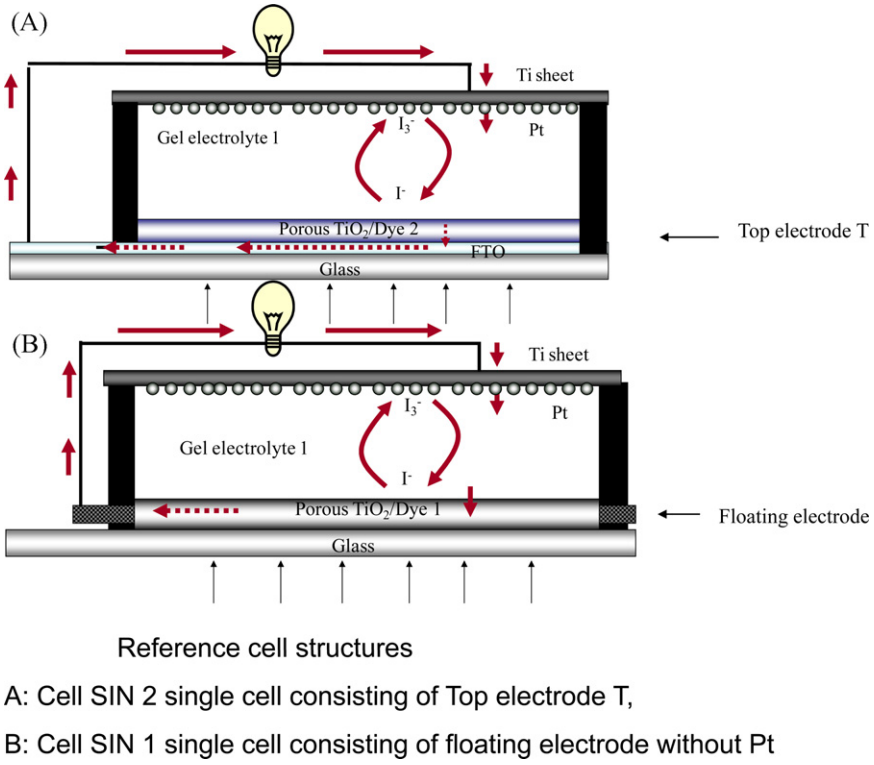

Fig. 7. Reference cell structures. A: Cell SIN 2 single cell consisting of top electrode T, B: Cell SIN 1 single cell consisting of bottom electrode B without Pt.

shown in Fig. 6B was prepared by assembling a cover glass substrate (thickness: 1 mm), a bottom electrode B, a gel electrolyte sheet 2, and a Ti sheet with Pt catalyst layer.

Photovoltaic performance was monitored with a Bunko-Keiki simulator KHP-1 equipped with a xenon lamp (XLS-150A). The exposure light was adjusted to be AM1.5 (100 mW/cm^2). The solar simulator spectra and power were adjusted using an Eiko Seiki solar simulator spectroradiometer LS-100. Exposure power was also corrected with an amorphous Si photodetector (Bunko-Keiki BS-520 S/N 007), which has visible-light sensitivity similar to that of DSC. After the cell fabrication, cell area was precisely recalculated using the obtaining photograph image. A mask was used for the evaluation. Spectra of light passing from a top electrode T or a Pt layer were monitored by an Eiko Seiki solar simulator spectroradiometer LS-100.

3. Results and discussion

3.1. Structure of Cell TAN and working principle

Fig. 1 shows a Cell TAN consisting of the floating electrode. The top electrode T consists of a porous titania layers stained with dye 2 covering a short wavelength region. The bottom electrode B is a floating electrode consisting of a porous titania/dye 1 layer supported by a stainless steel mesh. The floating electrode is a self-standing flexible sheet and can be handled easily. Light is introduced from the front side and is absorbed by a top electrode T, followed by a bottom electrode B. The expected working principle is shown in Fig. 2. The charge separation occurs at a titania/dye 2 layer in a top electrode T. Electron is collected by a FTO glass and is directed to a counter Ti sheet electrode. Electron is injected into iodine in a gel electrolyte 2 with the aid of Pt catalyst. Electron is carried by iodide and is given to an oxidized dye 1 in a bottom electrode B. Dye 1 in a bottom electrode B is photo-excited by light passing through a top electrode T and a gel electrolyte 1 layer. The photo-excited electron is injected into a titania layer in a bottom electrode B. Electron shifts from a titania layer to iodine in a gel electrolyte 1 with the aid of Pt catalyst which was deposited on the surface of the bottom electrode B. Iodide ion again carries electrons in the gel electrolyte 1. Finally the electron shifts from iodide ions to an oxidized dye 2 in a top electrode T.

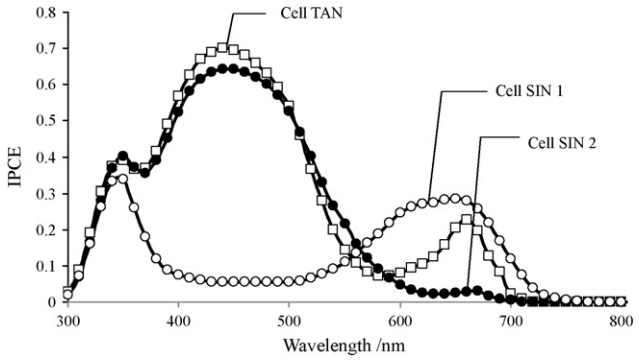

Fig. 8. IPCE curves for Cell TAN, SIN1 and SIN 2.

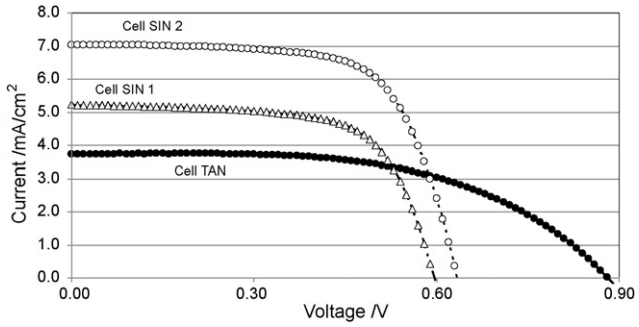

Fig. 9. *I–V* curves for Cell TAN, SIN1 and SIN 2. Cell structures: see Fig. 1 for Cell TAN, Fig. 7B for Cell SIN2, and Fig. 7A for Cell SIN 1.

3.2. Photovoltaic performance of Cell TAN

Fig. 8 shows Incident Photon to Current Efficiency (IPCE) curves for Cell TAN, Cell SIN 1 (single cell) and Cell SIN 2 (single cell). The Cell TAN had two peaks (450 nm and 660 nm) which corresponded to those of Cell SIN 2 and Cell SIN 1. Fig. 9 shows photovoltaic performances for these cells. Short circuit current density (J_{sc}) and open circuit voltage (V_{oc}) for Cell TAN were 3.72 mA/cm^2 and 0.88 V, respectively. V_{oc} of Cell TAN was higher than those of the corresponding single sells, 0.64 V of Cell SIN 2 and 0.60 V of Cell SIN 1. J_{sc}

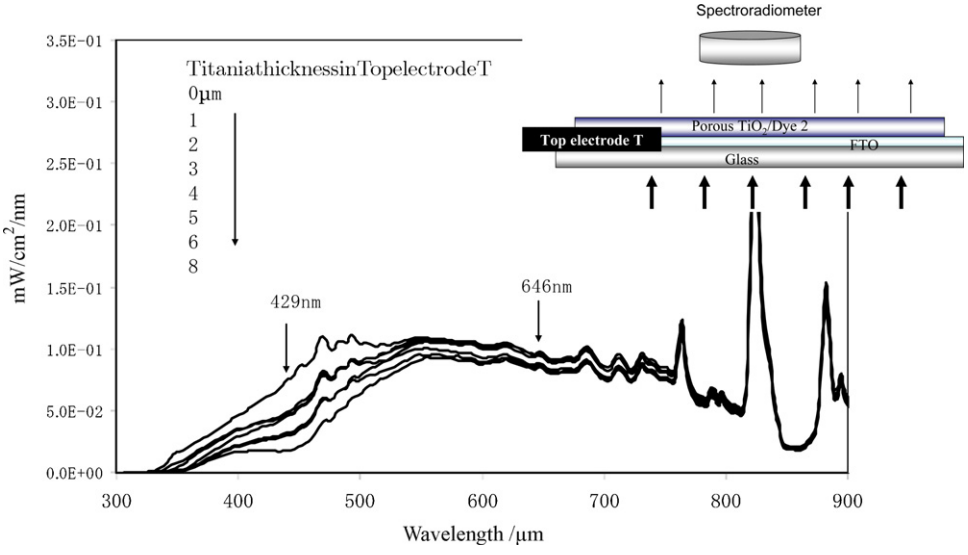

Fig. 10. Spectra of light after light passed through top electrode T. TiO_2 thickness in top electrode T was varied.

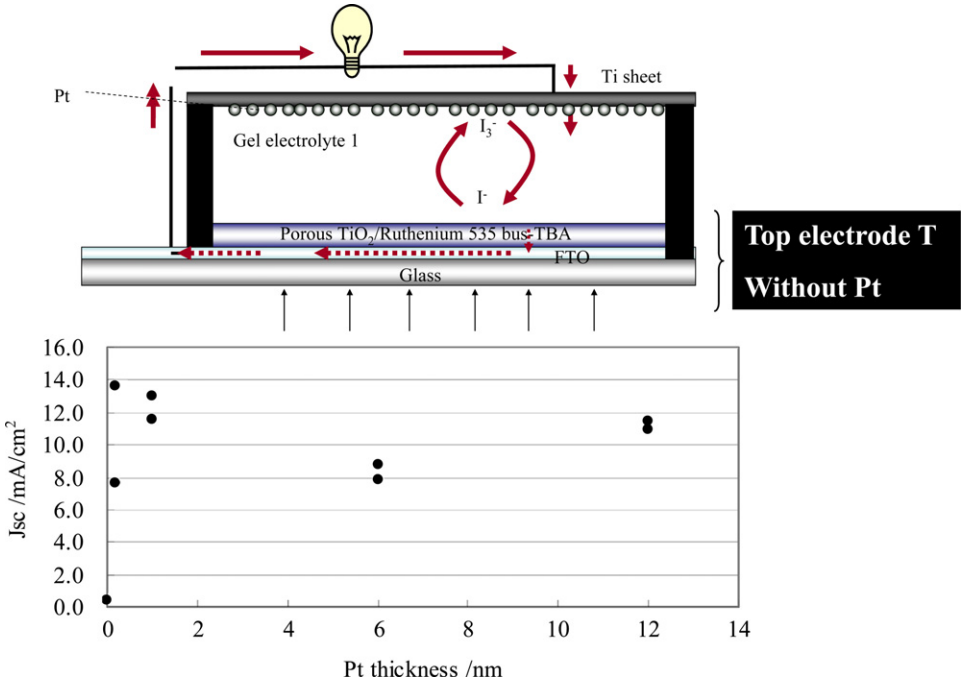

Fig. 11. Relationship between J_{sc} and Pt thickness of counter electrode. Cell SIN 2 was used for this experiment. A cis-diisothiocyanato-bis(2,2′-bipyridyl-4,4′-dicarboxylato) ruthenium(II) bis (tetrabutylammonium) (Ruthenium 535 bis-TBA, Solaronix) was used for dye-staining of titania layer.

of Cell TAN was 3.72 mA/cm^2, which was lower than 7.0 mA/cm^2 of Cell SIN 2 and 5.2 mA/cm^2 of Cell SIN 1. Optimization of these electrodes is needed so that J_{sc} of Cell SIN2 would be the same as that of Cell SIN 1. However, the facts that the IPCE curve had two peaks and the V_{oc} is higher than those of these single cells demonstrated clearly that the Cell TAN has a potential for tandem cells.

Fig. 10 shows spectra of lights after passing through a top electrode T, where, the thickness of the top electrode T was varied from 0 μm to 8 μm. The spectrum curve at 429 nm assigned to the absorption of dye 2 decreased with an increase in the titania layer thickness. However, the spectrum curve at 646 nm assigned to that of dye 1 did not change largely even when the titania thickness of the top electrode T increased. This means that the light passed the highly transparent titania layer and reach the dye 2. This is because the titania layer did not contain light-scattering particles which are conventionally employed for high-efficiency single cells.

3.3. Relationship between Pt layer thickness and photovoltaic performances

A most serious problem was light absorption loss caused by a Pt layer deposited on the surface of the bottom electrode B. Short circuit current density (J_{sc}) was affected significantly by the Pt thickness. Fig. 11 shows the relationship between J_{sc} and Pt thickness when the Pt thickness of Cell SIN 2 was varied. J_{sc} saturated at only 0.2–1.0 nm thickness of Pt layer, suggesting that less than

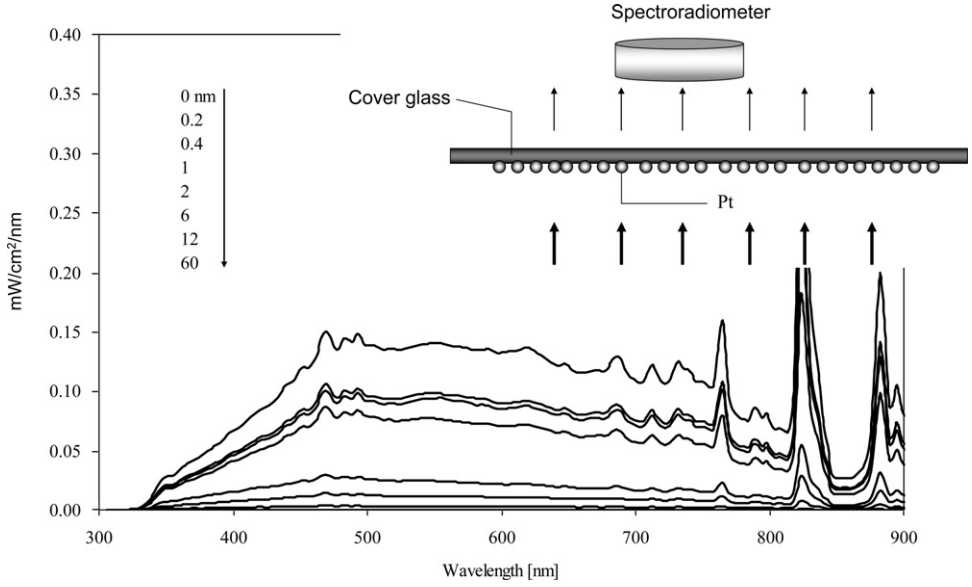

Fig. 12. Spectra of solar light after the solar light (AM 1.5, 100 mW/cm^2) passed through a flat glass on which Pt layer was deposited. The thickness of the Pt layer was varied.

1.0 nm thickness of Pt layer is enough for the full catalytic activity. Fig. 12 shows spectra of solar light (AM 1.5, 100 mW/cm^2) after the solar light passed through a flat glass on which a Pt layer was deposited. The light intensity decreased with an increase in a Pt layer thickness and the light did not pass through a Pt layer with 12 nm thickness. 1/3 of the solar light was lost after the solar light was passed through 1 nm thickness of Pt layer which was deposited in our deposition condition. J_{sc} of Cell TAN was lower than those of the corresponding single cell probably because Pt layer on the surface of the bottom electrode B disturbed light harvesting properties of the bottom electrode B. Improvement of the light transmittance through the Pt layer is crucial in order to increase the efficiency.

4. Conclusion

Tandem cell was prepared by inserting a floating electrode between a cathode and an anode of a conventional dye-sensitized solar cell. The V_{oc} of the Cell TAN was 0.88 V which was much higher than that of the corresponding single cell (0.6 and 0.66 V) and IPCE curve had two peaks corresponding to those of single cells. J_{sc} of the Cell TAN was lower than those of the corresponding single cell probably because Pt layer on the surface of the bottom electrode B disturbed the light harvesting properties of the bottom electrode B. Light transmittance through Pt layer on the bottom electrode B should be improved in order to increase the tandem cell performance. We need to optimize the cell structure, however, it was proved that the Cell TAN structure can be prepared easily and has a potential for tandem cells.

References

[1] B. O'Regan, M. Grätzel, Nature 353 (1991) 737.
[2] M.A. Green, K. Emery, D.L. King, Y. Hishikawa, W. Warta, Prog. Photovolt.: Res. Appl. 14 (2006) 455.
[3] M.K. Nazeeruddin, A. Kay, I. Rodicio, R. Humphry-Baker, E. Muller, P. Liska, N. Vlachopoulos, M. Grätzel, J. Am. Chem. Soc. 115 (1993) 6382.
[4] T. Renouard, R.-A. Fallahpour, M.K. Nazeerudin, R. Humphry-Baker, S.I. Gorelsky, A.B.P. Lever, M. Grätzel, Inorg. Chem. 41 (2002) 367.
[5] R. Amadelli, R. Argazzi, C.A. Bignozzi, F. Scandola, J. Am. Chem. Soc. 112 (1990) 7099.
[6] Z.-S. Wang, C.-H. Huang, B.-W. Zhang, Y.-Y. Hou, P.-H. Xie, H.-J. Qian, K. Ibrahim, New J. Chem. 24 (2000) 567.
[7] Y. Chiba, A. Islam, Y. Watanabe, R. Komiya, N. Koide, L. Han, Jpn. J. Appl. Phys. 45 (2006) L638.
[8] M.K. Nazeeruddin, P. Pechy, T. Renouard, S.M. Zakeeruddin, R. Humphry-Baker, P. Comte, P. Liska, L. Cevey, E. Costa, V. Shklover, L. Spiccia, G.B. Deacon, C.A. Bignozzi, M. Grätzel, J. Am. Chem. Soc. 123 (2001) 1613.
[9] Z.-S. Wang, T. Yamaguchi, H. Sugihara, H. Arakawa, Langmuir 21 (2005) 4272.
[10] M. Gratzel, J. Photochem. Photobiol. A 164 (2004) 3.
[11] P. Wang, S.M. Zakeeruddin, P. Comte, R. Charvet, R. Humphry-Baker, M. Grätzel, J. Phys. Chem. B 107 (2003) 14336.
[12] F. Gao, Y. Wang, J. Zhang, D. Shi, M. Wang, R.H. -Baker, P. Wang, S.M. Zakeeruddin, M. Grätzel, Chem. Commun. (2008) 2635.
[13] P. Liska, K.R. Tampi, M. Graetzel, D. Bremaud, D. Rudmann, H.M. Upadhyaya, A.N. Tiwari, Appl. Phys. Lett. 88 (2006) 203103.
[14] W. Kubo, A. Sakamoto, T. Kitamura, Y. Wada, S. Yanagida, J. Photochem. Photobiol. A: Chem. 164 (2004) 33.
[15] M. Dürr, A. Bamedi, A. Yasuda, G. Nelles, Appl. Phys. Lett. 84 (2004) 3397.
[16] M. Murayama, T. Mori, J. Phys. D 40 (2007) 1664.
[17] F. Inakazu, Y. Noma, Y. Ogomi, S. Hayase, Appl. Phys. Lett. 93 (2008) 093304.
[18] J. He, H. Lindström, A. Hagfeldt, S.-E. Lindquist, Sol. Energy Mater. Sol. Cells 62 (2000) 265.
[19] F. Vera, R. Schrebler, E. Muñoz, C. Suarez, P. Cury, H. Gómez, R. Córdova, R.E. Marotti, E.A. Dalchiele, Thin Solid Films 490 (2005) 182.
[20] F. Inakazu, Y. Noma, Y. Ogomi, S. Hayase, Appl. Phys. Lett. 92 (2008) 033308.
[21] Y. Yoshida, S.S. Pandey, K. Uzaki, S. Hayase, M. Kono, Y. Yamaguchi, Appl. Phys. Lett. 94 (2009) 093301.